

(Draft version)

# Broadband THz Interconnect for Hybrid Integration of InP and Si Platforms

Shuya Iwamatsu<sup>1</sup>, Muhsin Ali<sup>2</sup>, Jose Luis Fernandez-Estevez<sup>1</sup>, Sumer Makhoul<sup>1</sup>,  
Guillermo Carpintero<sup>2</sup>, and Andreas Stöhr<sup>1</sup>

<sup>1</sup>University of Duisburg-Essen, ZHO, Lotharstr. 55, 47057 Duisburg, Germany

<sup>2</sup>Universidad Carlos III de Madrid, Avenida de la Universidad 30, 28911 Leganés, Madrid, Spain

**Abstract**—We demonstrate a broadband terahertz coupling between InP-based coplanar waveguide and silicon dielectric rod waveguide for hybrid integration. A coupling efficiency of around -2 dB has been experimentally achieved in frequency range between 70-120 GHz. Numerical simulations reveal an operational 3dB-bandwidth >100 GHz.

## I. INTRODUCTION

**B**roadband operation in the THz frequency range has been demanded for many applications, such as THz spectroscopy, radar, and communication [1]. Photomixing using a uni-traveling-carrier photodiode (UTC-PD) [2] is one of the most promising candidates for ultra-wideband THz sources because the operation frequency can simply be tuned by changing the differential frequency from a dual laser source. To utilize the broadband feature of photomixers, we need a wideband input/output interface that can be monolithically integrated with state-of-the-art InP based THz UTC-PDs [2-4]. In this respect, a dielectric rod waveguide (DRW) made of high-permittivity material such as high-resistivity silicon (Si) has attracted increased attention due to its low loss and ultra-broadband operational bandwidth [5].

This paper presents a THz coupler for interconnecting the coplanar waveguide (CPW) output of THz UTC-PDs to a Si-based DRW. The coupler consists of an InP-based tapered-slot mode converter. Broadband coupling between the InP-based planar waveguide and the Si rod waveguide is demonstrated from numerical and experimental results.

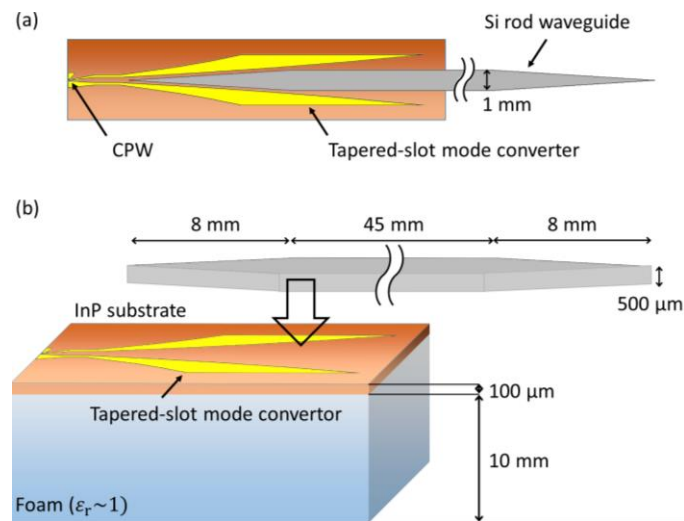


**Fig. 1.** Schematic concept of THz coupler for interconnecting InP-based coplanar waveguide (CPW) ports and Si rod waveguides featuring tapered structures at both ends. The InP chip is mounted on a THz foam, ROHACELL® with a dielectric constant  $\sim 1$ . (a) Top view and (b) 3-D view of the studied THz coupler showing also the Si rod waveguide which is aligned in the center of the tapered-slot mode converter.

## II. DEVICE DESIGN AND FABRICATION

Figure 1 shows the concept of the THz coupler between the InP-based planar CPW and the Si rod waveguide. The coupler mainly consists of a transition from a coplanar waveguide to a coplanar stripline (CPS) followed by a 12-mm long tapered-slot mode converter on the 100- $\mu\text{m}$  thick InP substrate and the Si rod waveguide with a thickness of 500  $\mu\text{m}$ . The CPW input allows the integration with active components like THz UTC-PDs. The idea of the mode converter comes from a previous hybrid integration reported [6]. The signal fed from the source goes through the CPW-to-CPS transition and reaches the tapered-slot mode converter, which transfers the planar CPS mode to the fundamental mode of the 8-mm long taper of DRW. The DRW has the same 8-mm long taper on the other side to allow the low-loss coupling to various hollow waveguides, which is helpful for characterization within different THz frequency

bands and valuable for system integration at any frequency band.

For fabrication, the mode converter and the transition were metalized on the InP substrate and bonded to a foam with an extremely low dielectric constant ( $\epsilon_r \sim 1$ ), ROHACELL® HF in the THz domain, as shown in Fig. 2. As a bonding layer, a Benzocyclobutene polymer (BCB) was used. The dielectric constants of the foam ( $\sim 1$ ) and of the BCB (2.65) are both lower than that of InP (12.4), which is required to keep the effective thickness of the substrate thin to suppress the substrate modes and reduce the dielectric loss of the coupler. The DRW was fabricated from a 500- $\mu\text{m}$  thick Si wafer using a deep reactive ion etching (DRIE) process.

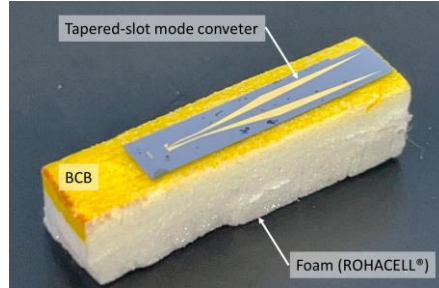


**Fig. 2.** Photograph of the fabricated InP-based tapered-slot mode converter with 100- $\mu\text{m}$  thickness on the foam (ROHACELL®). The InP chip was bonded on the foam with Benzocyclobutene polymer (BCB) (yellow-colored).

### III. EXPERIMENTAL RESULTS AND SIMULATIONS

To evaluate the coupling efficiency of the fabricated coupler, we measured the S-parameters ( $S_{21}$ ) of the coupler using a vector network analyzer (VNA) from 60 to 90 GHz, as shown in Fig. 3 (a). The mode converter is excited by a ground-signal-ground (GSG) probe, and the output from the Si taper is detected by another THz coupler (V-coupler) [7], fabricated on a commercial substrate. First, we measured the response of the V-coupler in a back-to-back configuration for reference. Afterward, the coupling efficiency from the InP-based CPW port to the DRW (see green lines in Fig. 4) was experimentally determined. For the coupling efficiency from 90 to 120 GHz, a UTC-PD featuring a rectangular hollow waveguide output was used as the THz source instead of the VNA (Fig. 3(b)). The mode converter was excited by a hollow waveguide to the GSG probe, and the output from the Si taper was detected by a power meter (Erickson PM5). After the photodiode's response was measured for reference, the insertion loss of the fabricated THz coupler was measured and evaluated (see red line in Fig. 4). The overall results show a decent coupling efficiency of around -2 dB, starting from the lower cut-off frequency at around 65 GHz. From Fig. 4, some fluctuations can be

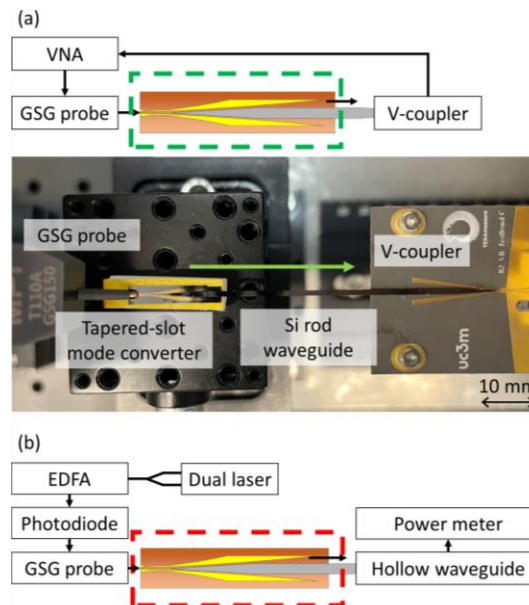


**Fig. 3.** Experimental setups for measuring the coupling efficiency of the fabricated coupler using (a) the Vector Network Analyzer (VNA) within 60-90 GHz and (b) a UTC-PD and a THz power meter for 90-120 GHz. (GSG: Ground-signal-ground, EDFA: Erbium-doped fiber amplifier)

observed, which are traced back to an imperfect probe contact and remaining standing waves between multiple components in the setup.

Comparing the measurements to the simulated results using the full-wave electromagnetic-wave simulation tool CST Studio Suite 2021, the better coupling efficiency is observed at around 75 GHz. This is expected to be caused by the non-perfect GSG probe calibration, which causes the error when de-embedding the probe's losses for determining the coupling efficiency from the measurements. Despite that, the cut-off frequency around 65 GHz agrees very well between the simulation and the measurement. The simulated results show a minimum coupling loss of about -1.5 dB at 108 GHz and indicate the fabricated THz coupler has an operational 3dB-bandwidth above 100 GHz.

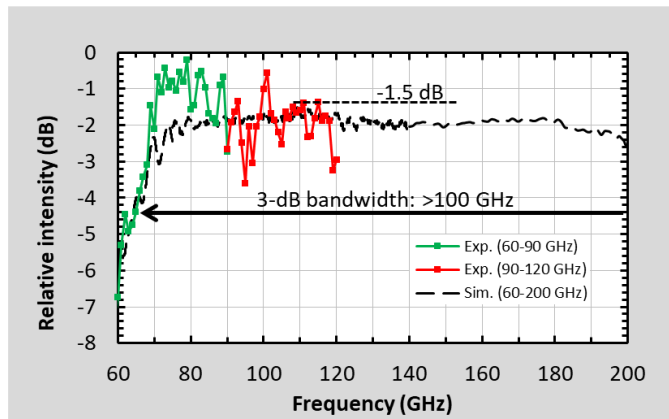


Fig. 4. Measured coupling efficiency of the fabricated coupler between 60 to 90 GHz (green) and between 90 to 120 GHz (red). The black line represents the simulated coupling efficiency using CST Studio Suite. According to simulations, the 3dB-bandwidth exceeds 100 GHz.

#### IV. SUMMARY

We proposed a broadband THz interconnect using an InP-based tapered-slot mode converter for transferring the planar waveguide mode into the fundamental mode of a Si dielectric rod waveguide. The use of a Si rod taper enables a low-loss connection to any rectangular-waveguide-based components. Experimentally, a coupling loss of only -2 dB has been achieved. According to CST simulations, the operational 3dB-bandwidth of the proposed THz coupler is expected to be over 100 GHz. The proposed approach allows monolithic integration of THz UTC-PDs to a broadband coupling interface.

#### REFERENCES

- [1]. P. H. Siegel, "Terahertz technology," in *IEEE Transactions on Microwave Theory and Techniques*, vol. 50, no. 3, pp. 910-928, March, 2002.
- [2]. T. Ishibashi, N. Shimizu, S. Kodama, H. Ito, T. Nagatsuma and T. Furuta, "Uni-traveling-carrier photodiodes," *Tech. Dig. Ultrafast Electronics Optoelectronics OSA Spring Topical Meeting*, pp. 166-168, 1997.
- [3]. B. Khani, S. Makhoulouf, A. G. Steffan, J. Honecker and A. Stöhr, "Planar 0.05–1.1 THz Laminate-Based Transition Designs for Integrating High-Frequency Photodiodes With Rectangular Waveguides," in *Journal of Lightwave Technology*, vol. 37, no. 3, pp. 1037-1044, Feb., 2019.
- [4]. T. Kurokawa, T. Ishibashi, M. Shimizu, K. Kato and T. Nagatsuma, "Over 300 GHz bandwidth UTC-PD module with 600 GHz band rectangular-waveguide output," *Electron. Lett.*, vol. 54, no. 11, pp. 705-706, May, 2018.
- [5]. A. Rivera-Lavado, S. Preu, L. E. García-Muñoz, A. Generalov, J. Montero-de-Paz, G. Döhler, et al., "Dielectric Rod Waveguide Antenna as THz Emitter for Photomixing Devices," *IEEE Transactions on Antennas and Propagation*, vol. 63, no. 3, pp. 882-890, Mar., 2015.
- [6]. X. Yu, J.-Y. Kim, M. Fujita, and T. Nagatsuma, "Efficient mode converter to deep-subwavelength region with photonic-crystal waveguide platform for terahertz applications," *Opt. Express* 27, pp. 28707-28721 2019.
- [7]. M. Ali, et al., "Dielectric Rod Waveguide-based Radio-Frequency interconnect operating from 50 GHz to 340 GHz," *2022 47th International Conference on Infrared, Millimeter, and Terahertz Waves (IRMMW-THz)*, 2022. (Accepted)

# DuEPublico

Duisburg-Essen Publications online

UNIVERSITÄT  
DUISBURG  
ESSEN

Offen im Denken

ub | universitäts  
bibliothek

This text is made available via DuEPublico, the institutional repository of the University of Duisburg-Essen. This version may eventually differ from another version distributed by a commercial publisher.

**DOI:** 10.1109/IRMMW-THz50927.2022.9895647

**URN:** urn:nbn:de:hbz:465-20230330-163358-3

This is the **authors version** of: S. Iwamatsu, M. Ali, J. L. Fernandez-Estevez, S. Makhlof, G. Carpintero and A. Stöhr, "Broadband THz Interconnect for Hybrid Integration of InP and Si Platforms," in: *2022 47th International Conference on Infrared, Millimeter and Terahertz Waves (IRMMW-THz)*, Delft, Netherlands, 2022. doi: 10.1109/IRMMW-THz50927.2022.9895647.

Personal use of this material is permitted. Permission from IEEE must be obtained for all other uses, in any current or future media, including reprinting/republishing this material for advertising or promotional purposes, creating new collective works, for resale or redistribution to servers or lists, or reuse of any copyrighted component of this work in other works.

© 2022, IEEE. All rights reserved.